ACS APPLIED MATERIALS & INTERFACES

Research Article

www.acsami.org

Bioinspired Near-Infrared-Excited Sensing Platform for in Vitro Antioxidant Capacity Assay Based on Upconversion Nanoparticles and a Dopamine–Melanin Hybrid System

Dong Wang,[†,‡,§] Chuan Chen,[†,§] Xuebin Ke,[‡] Ning Kang,[‡] Yuqing Shen,[⊥] Yongliang Liu,[‡] Xi Zhou,[‡] Hongjun Wang,[∥] Changqing Chen,[¶] and Lei Ren*[,†,‡]

[†]State Key Laboratory for Physical Chemistry of Solid Surfaces, Department of Chemistry, College of Chemistry and Chemical Engineering, and [‡]Department of Biomaterials, College of Materials, Xiamen University, Xiamen 361005, P. R. China

[⊥]Department of Blood Transfusion, Xiamen Maternity & Child Healthcare Hospital, Xiamen 361005, P. R. China

[∥]Department of Chemistry, Chemical Biology, and Biomedical Engineering, Stevens Institute of Technology, Hoboken, New Jersey 07030, United States

[¶]Department of Orthopaedic Surgery, The Affiliated Southeast Hospital of Xiamen University, Orthopaedic Center of People's Liberation Army, Zhangzhou 363000, P. R. China

Supporting Information

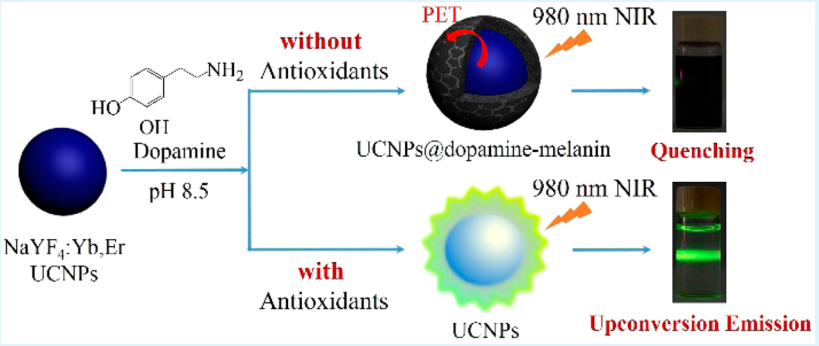

ABSTRACT: A novel core–shell structure based on upconversion fluorescent nanoparticles (UCNPs) and dopamine–melanin has been developed for evaluation of the antioxidant capacity of biological fluids. In this approach, dopamine–melanin nanoshells facilely formed on the surface of UCNPs act as ultraefficient quenchers for upconversion fluorescence, contributing to a photoinduced electron-transfer mechanism. This spontaneous oxidative polymerization of the dopamine-induced quenching effect could be effectively prevented by the presence of various antioxidants (typically biothiols, ascorbic acid (Vitamin C), and Trolox). The chemical response of the UCNPs@dopamine–melanin hybrid system exhibited great selectivity and sensitivity toward antioxidants relative to other compounds at 100-fold higher concentration. A satisfactory correlation was established between the ratio of the "anti-quenching" fluorescence intensity and the concentration of antioxidants. Besides the response of the upconversion fluorescence signal, a specific evaluation process for antioxidants could be visualized by the color change from colorless to dark gray accompanied by the spontaneous oxidation of dopamine. The near-infrared (NIR)-excited UCNP-based antioxidant capacity assay platform was further used to evaluate the antioxidant capacity of cell extracts and human plasma, and satisfactory sensitivity, repeatability, and recovery rate were obtained. This approach features easy preparation, fluorescence/visual dual mode detection, high specificity to antioxidants, and enhanced sensitivity with NIR excitation, showing great potential for screening and quantitative evaluation of antioxidants in biological systems.

KEYWORDS: *upconversion nanoparticles, dopamine, melanin, biothiols, antioxidant capacity assay, near-infrared*

INTRODUCTION

Oxidative stress, defined as the imbalance between the production of reactive oxygen and nitrogen species (ROS/RNS) and the endogenous antioxidant defense network,[1] plays a pivotal role in different pathophysiological conditions,[2] such as cardiovascular disease,[3] mild cognitive impairment,[4] Alzheimer's disease,[5] Parkinson's disease,[6] and certain types of cancer.[7] Living organisms have developed complex antioxidant systems to counteract reactive species in the defense network for reducing their damage.[8] These antioxidants comprise of various macromolecules, enzymes, and small molecules, such as reduced glutathione (GSH), cysteine

Received: September 4, 2014
Accepted: January 21, 2015
Published: January 21, 2015

DOI: 10.1021/am5086269
ACS Appl. Mater. Interfaces 2015, 7, 3030–3040

(Cys), ascorbic acid (AA or Vc), α-tocopherol, β-carotene, ubiquinol-10, methionine, and bilirubin.[9] Increasing epidemiological studies suggest that the intake of an antioxidant-rich diet may inversely correlate with the risk of developing pathologies such as cardiovascular diseases and cancers.[10,11] Although this proposal remains controversial, significant attention has been drawn to the antioxidant capacity assay of natural products and their relationships with an endogenous antioxidant defense system.[12,13]

Because of the synergistic interactions among different antioxidant components in biological fluids and the difficulty of measuring individual antioxidant components, one of the most common strategies to assess the free-radical-antioxidant balance in biological systems is to determine the total antioxidant capacity.[8,12,14] Various methods have been developed to investigate the antioxidant capacity of body fluids, food, vegetable extracts, and beverages.[12,13,15] These include 6-hydroxy-2,5,7,8-tetramethylchroman-2-carboxylic acid (Trolox)-equivalent antioxidant capacity (TEAC) assay,[14] ferric-reducing antioxidant power assay,[16] and competitive reaction methods, such as oxygen radical absorbance capacity assay[17] and total radical-trapping antioxidant parameter assay.[18] These assays are mainly based on spectrophotometric analysis. Besides the chemical instability of the used organic probes, these detections often suffer from inevitable autofluorescence or strong background light absorption due to the presence of interfering biomolecules, which can also be excited by ultraviolet (UV) or near-UV light, resulting in a low signal-to-noise ratio of detection.[19,20]

More recently, novel strategies for antioxidant capacity evaluation based on nanoparticles (NPs) and nanotechnology have been proposed.[21] Some gold NP-based optical methods for antioxidant functional evaluation have been achieved.[22,23] Other sensing strategies based on silver NPs or quantum dots (QDs) have also been developed for quick detection of the analytes with free-radical scavenging capability.[24−26] The unique localized surface plasmon resonance optical property of noble metal NPs and the size-dependent fluorescent emission of QDs identify them as a new generation of optical labels.[27] Compared with the organic probes, NPs are more chemically stable and can be easily conjugated with biomolecule or targeting ligands to achieve specific recognition in a biological environment. However, the strong background light absorption or autofluorescence interference in real sample analysis is still present with these NP-based spectrophotometric assays.

Upconversion nanoparticles (UCNPs), which can convert near-infrared (NIR) radiation to visible fluorescence, are emerging as a new generation of fluorescence biolabels.[28−30] Because of the NIR excitation, the signal-to-noise ratio and sensitivity in quantitative analysis are markedly enhanced owing to the absence of autofluorescence and scattering light from biological samples.[31] In particular, NIR irradiation has deeper penetration capability and is less harmful to biological samples compared to UV excitation. This is particularly valuable for in vivo biolabeling and biosensing assays.[32,33] To date, many studies have reported the detection of adenosine triphosphate, ions, protein, and amino acid based on fluorescence resonance energy transfer using UCNPs as energy donors to various acceptors including graphene oxide,[34] organic dyes,[35] gold NPs,[36] and MnO_2 nanosheets.[37] To our best knowledge, there is no exploration yet in using UCNPs for the antioxidant capacity determination of biological samples.

Melanins are a class of well-known biomacromolecules widely distributed in most living organisms.[38] Melanins exhibit a broad-band absorbance over the entire UV−vis region. Consistent with their role as potent photoprotectants and free-radical scavengers, melanins have been shown to efficiently deactivate >99.9% of absorbed UV and visible light photon energy through nonradiative means.[39] Inspired by the unique optoelectronic properties of melanins, we discovered that the upconversion fluorescence of UCNPs could be effectively quenched by the dopamine−melanin nanoshells in a weak alkaline buffer, as illustrated in Scheme 1. More importantly,

Scheme 1. Diagrammatic Illustration of the Mechanistic Principle of the Antioxidant Capacity Assay Platform Based on the UCNPs@Dopamine−Melanin Hybrid System

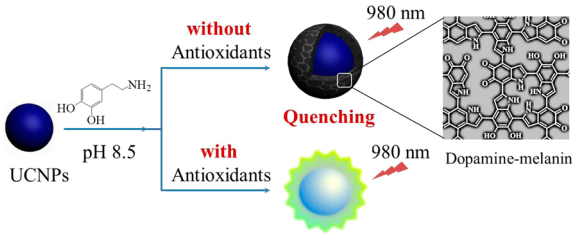

this spontaneous oxidative polymerization of the dopamine-induced quenching effect can be effectively inhibited by the presence of a variety of antioxidant substances, for example, GSH, Cys, Vc, Trolox, etc. Moreover, the "antiquenching" effect displayed a linear fluorescent response to a concentration range of antioxidants. Besides the fluorescence response, this antioxidant activity also showed a color change from colorless to dark gray accompanying the spontaneous oxidation of dopamine. Taking advantage of this bioinspired competitive spontaneous oxidative and antioxidative reaction system, a novel NIR-excited UCNP-based antioxidant capacity assay (UNACA) platform has been accordingly developed for in vitro evaluation of the antioxidant capacity of biological fluids.

RESULTS AND DISCUSSION

Characterization of UCNPs. In this study, β-$NaYF_4$:Yb,Er UCNPs were used as the fluorescence donor particularly because of its recognized high efficacy in NIR-to-visible upconversion up to now.[29] UCNPs were synthesized following a solvothermal procedure,[40] which was described in Experimental Section in detail. A transmission electron microscopy (TEM) image (Figure S1 in the Supporting Information, SI) showed that the obtained UCNPs had a uniform spherical morphology with an average particle size of 34.7 ± 2.9 nm. The crystal phase and structures were analyzed by X-ray diffraction (XRD) and exhibited well-defined diffraction peaks where the peak positions and intensities agreed well with the standard pattern of hexagonal $NaYF_4$ (Figure S2 in the SI), confirming the high quality of prepared UCNPs. Water-soluble UCNPs were subsequently prepared via surface ligand exchange of the oleic acid-capped hydrophobic UCNPs with sodium citrate in diethylene glycol (DEG) at a high temperature (200 °C).[41] Fourier transform infrared (FT-IR) spectra suggested that the surface oleic acid ligands were replaced successfully by citrate (Figure S3 in the SI). Surface ζ potential measurement further confirmed that the modified UCNPs were negatively charged with a potential of approximately −38.6 mV (Figure S4 in the

DOI: 10.1021/am5086269
ACS Appl. Mater. Interfaces 2015, 7, 3030−3040

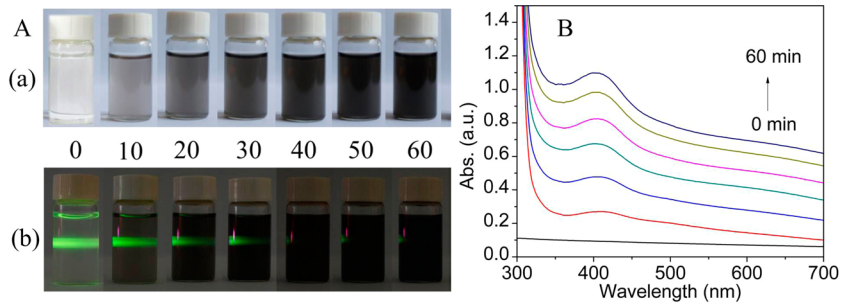

Figure 1. (A) Photographs of the UCNPs@dopamine−melanin hybrid system as the reaction time goes from 0 to 60 min, under natural light (a) and 980 nm NIR laser irradiation (b). (B) Evolution of UV−vis absorption spectra of the UCNPs@dopamine−melanin hybrid system with gradual formation of melanin via spontaneous oxidation of dopamine from 0 to 60 min. Samples were taken for testing per 10 min intervals.

SI), suggesting the high colloidal stability of UCNPs in a pH 8.5 Tris-HCl buffer solution.

Fluorescence Quenching of UCNPs by Spontaneous Oxidative Polymerization of Dopamine. Upon incubation of UCNPs with dopamine in a Tris-HCl buffer (pH 8.5), a color change of the solution from colorless to dark gray was observed as a function of time [Figure 1A(a)]. The process was monitored by UV−vis spectroscopy. As shown in Figure 1B, the broad and monotonic extended absorbance from the NIR to UV region represents the characteristic of synthetic melanin.[38] A continuous increase of the absorbance as a function of the reaction time was observed, indicating that dopamine−melanin was gradually formed in the mixed solution. Accompanied by the color change, an intensive fluorescence quenching on the upconversion emission of UCNPs with an increase of the reaction time was clearly seen in the dark [Figure 1A(b)] and quantitatively measured by fluorescence emission spectroscopy, as shown in Figure 2A. To

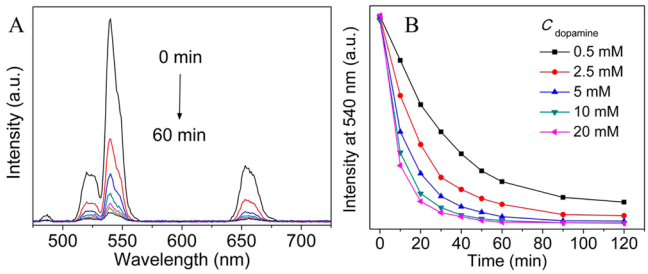

Figure 2. (A) Evolution of upconversion fluorescence spectra of UCNPs (0.2 mg/mL) upon incubation with dopamine hydrochloride (5 mM) in a Tris-HCl buffer (pH 8.5) solution from 0 to 60 min. Samples were collected for testing per 10 min intervals. (B) Plot of the fluorescence intensities recorded at 540 nm as a function of time from 0 to 120 min, in which UCNPs (0.2 mg/mL) were incubated with dopamine hydrochloride at different concentrations (0.5, 2.5, 5, 10, and 20 mM) in a Tris-HCl buffer.

obtain an optimized condition to perform sensing analysis, different concentrations (0.5, 2.5, 5, 10, and 20 mM) of dopamine were incubated with a fixed concentration of UCNPs (0.2 mg/mL). As depicted in Figure 2B, the quenching effect of dopamine−melanin toward UCNPs showed a concentration dependence when the concentration of dopamine was below 10 mM. This trend became less obvious in the concentration range from 10 to 20 mM. A rapid decrease of the fluorescence intensity was observed between 0 and 30 min when the concentration of dopamine was above 5 mM, and a plateau was reached for prolonged reaction time. To achieve a quick response while maintaining a broad efficient detection range, 5 mM dopamine per 0.2 mg/mL UCNPs and 30 min of preincubation time were used for further detection experiments.

The phenomenon that dopamine−melanin substantially quenched the fluorescence of UCNPs indicated a strong correlation between the excited state of UCNPs and the dopamine−melanin synthesis. Following photoexcitation, the energy-transfer upconversion process of $NaYF_4$:Yb,Er was well studied previously.[29] As shown in Figure 3, the sensitizer Yb^{3+}

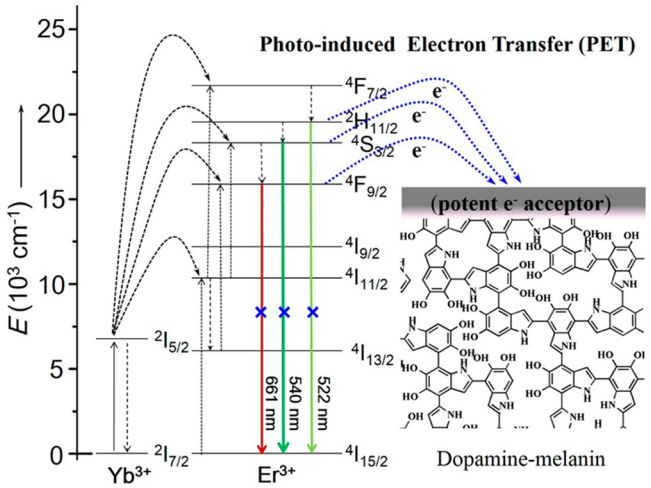

Figure 3. Proposed mechanism on the excitation and quenching of upconversion fluorescence by PET in the UCNPs@dopamine−melanin hybrid system.

can absorb the pump photons successively and then donate energy to activator Er^{3+}. The sequential absorption of photons by Er^{3+} populates the ions to the metastable level. Then, a nonradiative energy-transfer process promotes one of the ions in the metastable level to an upper emitting state, resulting in upconversion emission with three main peaks located at 522, 540, and 661 nm corresponding to the $^2H_{11/2} \rightarrow {}^4I_{15/2}$, $^4S_{3/2} \rightarrow {}^4I_{15/2}$, and $^4F_{9/2} \rightarrow {}^4I_{15/2}$ optical transitions,[29] respectively. After dopamine was added into the UCNP-containing Tris-HCl (pH 8.5) solution, it could be oxidized to quinone by the ROS, such as hydroxyl radical or dissolved oxygen, and finally to dopamine−melanin through complicated cross-linking reactions.[42] The active intermediates (quinones) and final product (dopamine−melanin) can function as favorable electron acceptors on the surface of UCNPs;[43,44] thus, the excited photoelectron of UCNPs will be instantaneously captured by

DOI: 10.1021/am5086269
ACS Appl. Mater. Interfaces 2015, 7, 3030−3040

quinones and melanin and may substantially dissipate as nonradiative heat. This process was similarly studied previously using photoacoustic calorimetry, in which eumelanin, especially at a higher molecular weight (M_w > 3000), could efficiently release approximately 90% of the absorbed photonic energy as heat.[45] This relaxation occurred in less than 20 ps as measured by a femtosecond pump−probe absorption study.[46] Therefore, the upconversion fluorescence process is eliminated because the excited electrons cannot return to the ground state, and the fluorescence of UCNPs is quenched most likely via the photoinduced electron-transfer (PET) mechanism.[47] This mechanism is consistent with the electrochemistry of dopamine−melanin and structurally related quinone molecules, known as potent electron acceptors in organisms.[48] To some extent, this observation agrees with previous findings that quinones and polydopamine could function as favorable electron acceptors for the photoexcited QDs,[43,44] porphyrin,[49] 6-carboxyfluorescein, and other fluorophores[50] to quench their fluorescence efficiently.

The formation of dopamine−melanin nanoshells on the UCNPs was further verified by TEM examination. As shown in Figure 4, a time-dependent growth of the shell layer on the surface of UCNPs was clearly seen. The thickness of the shell layer was about 2.6, 12.8, and 18.3 nm at the reaction time points of 10, 30, and 90 min, respectively. The deposition of a coating on various substances by the spontaneous oxidation of dopamine was first reported by Lee et al.,[42] and further examination of this process revealed that the composition of this polymerized coating was melanin.[51] The exact polymerization mechanism remains unclear, and it most likely occurs through spontaneous oxidation of dopamine to a quinone accompanying the intra/intermolecular cross-linking reactions in a manner reminiscent of melanin formation,[51,52] as shown in eq 1.

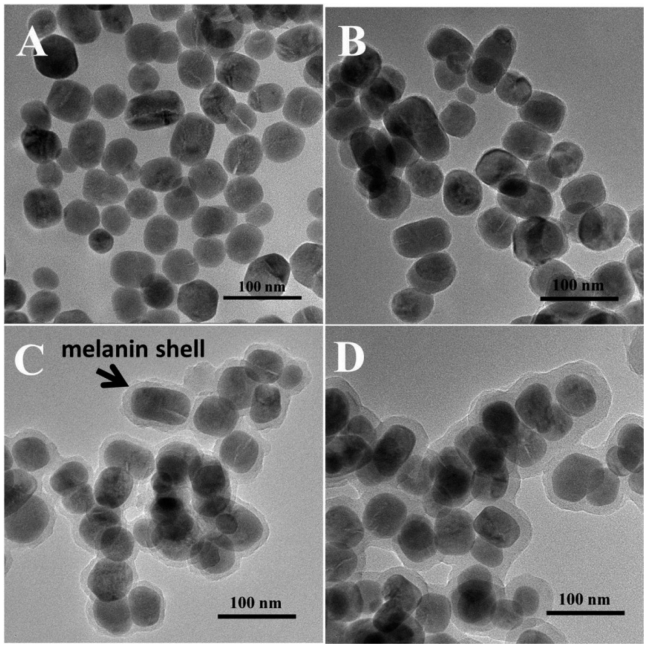

Figure 4. TEM images of the formation of dopamine−melanin nanoshells on the surface of UCNPs. The measurement was taken at the time points of 0 (A), 10 (B), 30 (C), and 90 min (D) after the addition of dopamine hydrochloride to the UCNP solution.

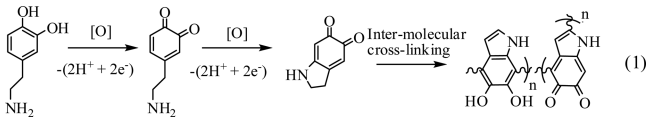

(1)

Antiquenching Effect of Various Antioxidants. With inspiration from the inhibition property of various endogenous antioxidants in melanin synthesis,[53,54] we believe that this spontaneous oxidative polymerization of dopamine can be effectively inhibited by the presence of a variety of antioxidants. To address this, GSH was first chosen as a model compound considering its abundance as an intracellular antioxidant in living organisms. The kinetic behaviors of the UCNPs@dopamine−melanin hybrid system with or without the presence of GSH were first investigated by UV−vis spectroscopy. In the absence of GSH, the absorbance of dopamine−melanin at 400 nm increased gradually (Figure 5A), suggesting the progress of self-polymerization of dopamine. With the presence of 20 μM GSH, the absorbance increased in a delayed manner, while with the 40 μM GSH, the absorbance remained at the baseline for more than 1 h. This reaction was also monitored by measuring the fluorescence emission of UCNPs at 540 nm (Figure 5B). In the absence of GSH, the fluorescence emission continuously decreased with the formation of dopamine−melanin, while the fluorescence intensity was retained with the addition of 40 μM GSH for the investigating times and decreased in a delayed manner with the addition of 20 μM GSH.

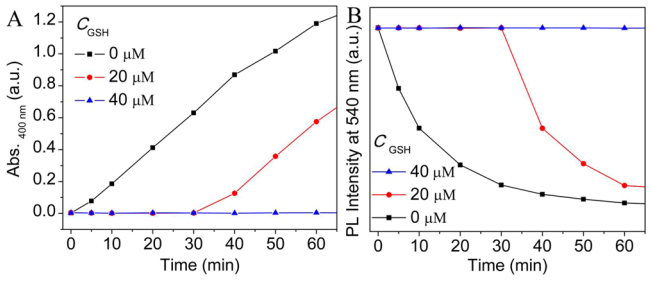

Figure 5. Time-resolved measurements of absorbance at 400 nm (A) and upconversion fluorescence intensity at 540 nm (B) of UCNPs@dopamine−melanin hybrid systems with the addition of 0, 20, and 40 μM GSH. Measurement was done per 10 min interval after the addition of dopamine hydrochloride (5 mM) to the UCNPs (0.2 mg/mL) containing a Tris-HCl (pH 8.5) solution.

GSH has an antioxidation property because of the fact that the thiol group in its Cys moiety is an active reducing agent, which can be reversibly oxidized and reduced. After the addition of GSH to the mixture of UCNPs and dopamine in a basic environment with dissolved oxygen, the thiol group of Cys is able to donate a reducing equivalent ($H^+ + e^-$) to other unstable molecules, such as ROS and free-radical intermediates, to terminate the spontaneous oxidation of dopamine by scavenging those unstable molecules and inhibiting other oxidation reactions. Upon donation of an electron, GSH itself becomes reactive and therefore readily reacts with another reactive GSH to form glutathione disulfide (GSSG) through thiol−disulfide exchange, as shown in eq 2. This antioxidation process goes efficiently and precisely in the present study so that 40 μM GSH can effectively inhibit the formation of dopamine−melanin within 1 h, leading to complete "anti-quenching" of the UCNP fluorescence intensity.

DOI: 10.1021/am5086269
ACS Appl. Mater. Interfaces 2015, 7, 3030−3040

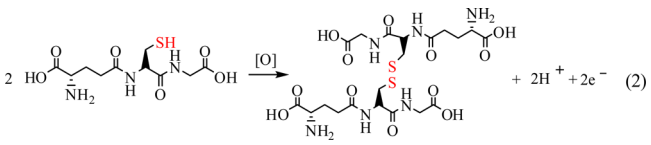

(2)

AA, which human beings obtain from the diet as vitamin C (Vc), is another important water-soluble antioxidant for living organisms. The antioxidant activity of Vc toward the UCNPs@dopamine−melanin hybrid systems was also investigated. The inhibition of dopamine−melanin synthesis by GSH, Cys, and Vc is shown in Figure 6A. The antioxidation reaction follows a

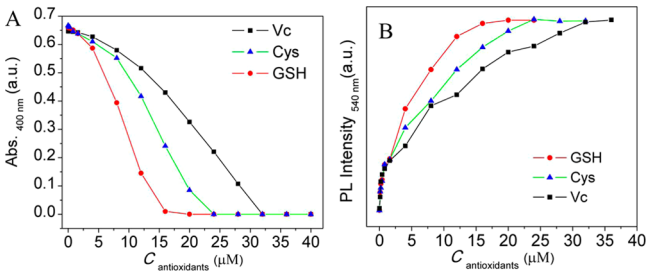

Figure 6. (A) Absorbance of the UCNPs@dopamine−melanin hybrid systems with the addition of a serial amount of GSH, Cys, and Vc showing the different inhibitive capabilities of GSH, Cys, and Vc toward dopamine oxidation reaction. (B) Corresponding upconversion fluorescence intensity at 540 nm of the samples with the same parameters as those in part A showing the different antiquenching effects of a serial amount of GSH, Cys, and Vc toward UCNPs. The test was carried out at 30 min of incubation time after the addition of different antioxidants to the mixture.

concentration-dependent manner, as measured by the absorbance of dopamine−melanin at 400 nm. The spontaneous oxidation of dopamine was completely inhibited when the concentrations of three antioxidants were above certain levels. These threshold values for GSH, Cys, and Vc are 15.5, 23.5, and 32 μM, respectively, when the initial concentration of dopamine was 5 mM and the reaction time was fixed at 30 min. Clearly, the antioxidation efficiency followed the order of GSH > Cys > Vc (Figure 6A). The ascorbate ion is the predominant species of Vc in a normal biological environment. When Vc was introduced into the reaction mixture, it promptly reacted with oxidants of the ROS, such as the hydroxyl radical, to complete the initiation of spontaneous oxidation polymerization of dopamine. Ascorbate can competitively terminate these oxidation reactions by electron transfer to form a radical cation and then dehydroascorbic acid with the loss of a second electron. The reaction is given in eq 3.

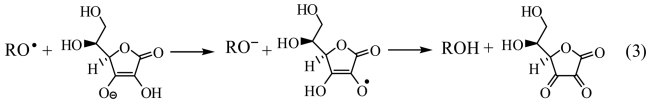

(3)

We also tested the antioxidant capacity of Trolox, a water-soluble analogue of vitamin E, which has been widely used as a standard in TEAC assays of body fluids, foods, beverages, and supplements.[14,16] As shown in Figure S5 in the SI, although Trolox showed an antioxidant manner similar to that of GSH, Cys, and Vc, the threshold value for complete inhibition of dopamine oxidation was about 50 mM, implying that the antioxidant capacity of Trolox was just about 0.1% that of Vc.

In accordance with the inhibition activity of GSH, Cys, and Vc in dopamine−melanin synthesis (Figure 6A), a synchronous change of the antiquenching effect of GSH, Cys, and Vc on the fluorescence emission of UCNPs was also recognized (Figure 6B). The antiquenching efficiency, corresponding to the antioxidant capacity, followed the order of GSH > Cys > Vc. This result indicates that the UCNPs@dopamine−melanin hybrid system can be used to evaluate the antioxidant capacity of the complex biological samples without autofluorescence background signal interference under 980 nm NIR excitation.

Antioxidant Capacity Assay in Aqueous Solution. On the basis of the above findings, quantitative evaluation of the antioxidant capacity in aqueous solution was performed using this UCNPs@dopamine−melanin hybrid system and GSH, Cys, and Vc were used as the representative model targets. UCNPs−dopamine was incubated with a series of antioxidants with increasing concentrations. The reaction was monitored by measuring the fluorescence emission of UCNPs after 30 min of reaction. The fluorescence spectra of UCNPs@dopamine−melanin in the presence of GSH with different concentrations are shown in Figure 7A. A gradual increase of the "antiquenching" upconversion fluorescence intensity was observed as the concentration of GSH increased from 0.2 to 20 μM. The original calibration curves for GSH, Cys, and Vc are given in Figure S6 in the SI. The "antiquenching efficiency" iss defined as $(F_n - F_0)/F_0$, where F_n is the fluorescence intensity of UCNPs at 540 nm in the presence of various concentrations of antioxidants and F_0 is the relative fluorescence intensity at 540 nm in the absence of antioxidants. It should be noted that the absorbance changes of the synthetic dopamine−melanin (Figure 6A) and antiquenching efficiency (Figure S6 in the SI) toward the concentration of antioxidants were not in a linear manner but followed a nonlinear allometric regression equation. An explanation of this interesting phenomenon will be addressed in future work. For convenience, the standard calibration curve of each antioxidant compound was linearized by taking the logarithm of $(F_n - F_0)/F_0$ and the concentration of antioxidants (nanomolar), respectively. The regression fit curves of GSH, Cys, and Vc are given in Figure 7B−D, a strong linear correlation was obtained between $\log[(F_n - F_0)/F_0]$ and $\log_{10}(C_{GSH})$, $\log(C_{Cys})$, or $\log(C_{Vc})$. The regression equation was $\log[(F_n - F_0)/F_0] = 0.461 \log(C_{GSH}) - 1.607$ ($R^2 = 0.996$) for GSH with a linear range from 0.1 to 20 μM; $\log[(F_n - F_0)/F_0] = 0.452 \log(C_{Cys}) - 1.663$ ($R^2 = 0.993$) for Cys with a linear range from 0.1 to 24 μM; $\log[(F_n - F_0)/F_0] = 0.379 \log(C_{Vc}) - 1.374$ ($R^2 = 0.985$) for Vc with a linear range from 0.1 to 32 μM, respectively. The results indicate that this UCNPs@dopamine−melanin hybrid system can be used to quantitatively detect GSH, Cys, and Vc or be used for evaluation of the total antioxidant capacity of a mixed sample by using GSH, Cys, Vc, or other antioxidants with a similar functional mechanism as standards. A 30 min incubation time seems necessary for the detection, and it should be considered as a viable strategy for in vitro antioxidant capacity assay of biological samples in recognition of the simplicity of the platform. Limited by the need for spontaneous oxidative polymerization of dopamine in a weak alkaline condition (set as pH 8.5 in the present study), the current system may not be suitable for intracellular detection or in vivo real-time monitoring yet. Our continuous efforts will be made to develop a detection system for living biological systems with physiological pH. On the other hand, the current bioinspired detection platform is designed more for

DOI: 10.1021/am5086269
ACS Appl. Mater. Interfaces 2015, 7, 3030−3040

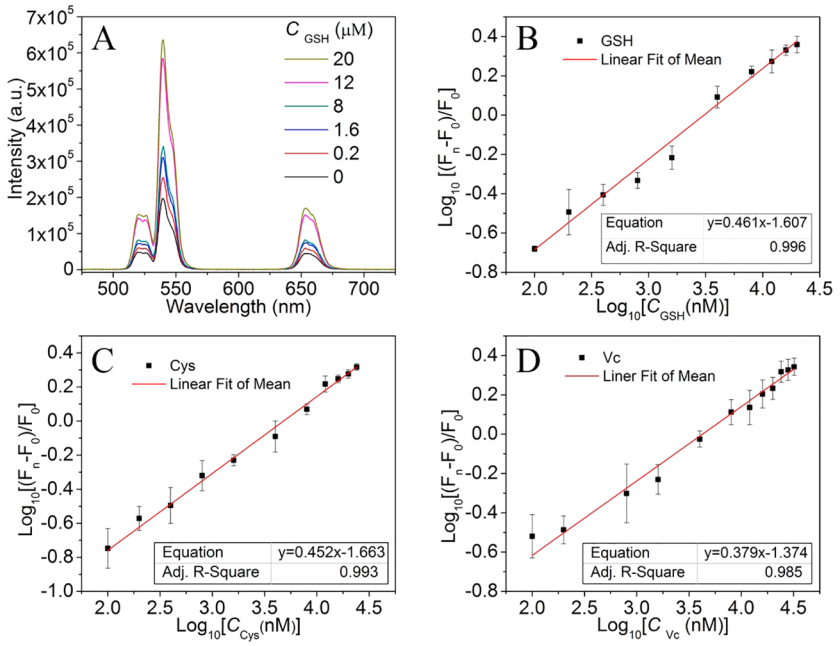

Figure 7. (A) Fluorescence spectra of the UCNPs@dopamine−melanin hybrid system as a function of the GSH concentration from 0 to 20 μM. (B−D) Linear plots of log(antiquenching efficiency) as a function of log(concentration of GSH, Cys, or Vc). The antiquenching efficiency is defined as $(F_n - F_0)/F_0$, where F_n is the fluorescence intensity of UCNPs at 540 nm in the presence of various concentrations of antioxidants and F_0 is the relative fluorescence intensity at 540 nm in the absence of antioxidants.

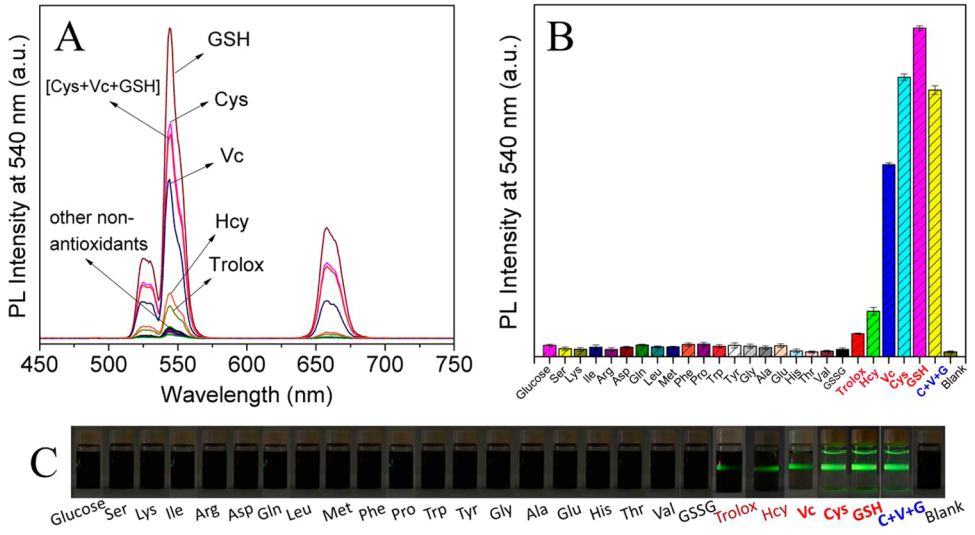

Figure 8. (A) Fluorescence spectra of the UCNPs@dopamine−melanin hybrid system upon incubation with 25 μM GSH, Cys, Hcy, Vc, Trolox, 76% Cys + 20% Vc + 4% GSH (C+V+G), and 100-fold excess (2.5 mM) of GSSG, glucose, and other common amino acids. (B) Relative photoluminescence intensities at 540 nm of the evaluation systems recorded in correspondence with the fluorescence spectra in part A. (C) Photographs of the samples in part A showing the differences in the color change and UC fluorescence intensity of the detection systems toward antioxidants and other compounds.

in vitro antioxidant capacity assay of biological fluids such as body fluid, in which the detection target of antioxidants can well maintain their activities in the pH 8.5 buffer. Additionally, this platform is also suitable for screening and evaluation of the antioxidants in food, vegetable extracts, and beverages.

Specificity of Antioxidant Capacity Assay. To further evaluate the specificity of the UCNPs@dopamine−melanin hybrid system for antioxidants, control experiments using glucose, GSSG, and a series of other amino acids at a 100-fold higher concentration (2.5 mM) than that of GSH, Cys, Hcy, Vc, and Trolox (25 μM) were performed to measure the upconversion fluorescence responses. As shown in Figure 8A, the change of the fluorescence intensity of the UCNPs@dopamine−melanin hybrid system in the presence of GSH, Cys, Hcy, and Vc was strikingly larger than that of other compounds. The "antiquenching" efficiency, corresponding to the antioxidation capability, followed the order of GSH > Cys > Vc > Hcy > Trolox ≫ GSSG, glucose, and other amino acids (Figure 8B). No obvious change in the quenched emission was observed with the addition of glucose, GSSG, and other amino acids in comparison to the blank controls. To assess the response of this detection platform toward a multicomponent

DOI: 10.1021/am5086269
ACS Appl. Mater. Interfaces 2015, 7, 3030−3040

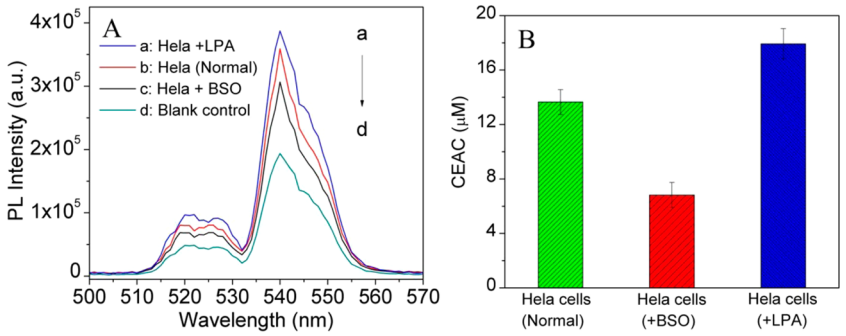

Figure 9. (A) Upconversion fluorescence response of the UCNPs@dopamine−melanin hybrid system toward nontreated and BSO (100 μM)- and LPA (500 μM)-preincubated Hela cells. (B) The relative CEAC value of each sample was calculated against the Cys calibration curve.

sample, a mixture with typical antioxidants in plasma (76% Cys + 20% Vc + 4% GSH)[55,56] was diluted with a MEM cell culture medium to obtain a simplified simulated body fluid at a final concentration of 25 μM and used for specificity testing following the same protocol. As can be seen in Figure 8, the mixed antioxidants showed a response similar to that of the Cys sample, and the antiquenching activity came from the summation of Cys, Vc, and GSH, indicating a satisfactory response of the UCNPs@dopamine−melanin hybrid system toward a mixed antioxidant sample. In addition to fluorescence analysis, the remarkable specificity for antioxidants over other compounds could be directly visualized from the differences in color and fluorescence intensity changes. The photographs taken from the solutions of the UCNPs@dopamine−melanin hybrid system in the presence of various antioxidants and other compounds are shown in Figure 8C. The antioxidants that inhibit the formation of dopamine−melanin result in colorless solutions under natural light and a strong upconversion fluorescence under 980 nm NIR irradiation, while the typical brownish-black melanin and almost completely quenched upconversion fluorescence were seen with the samples containing glucose, GSSG, or other amino acids. These results clearly demonstrated a high specificity of the current platform for the main antioxidants against other common amino acids and nonreducing compounds, indicating potential applications of the UCNPs@dopamine−melanin hybrid system for antioxidant capacity assay in biological samples.

Cytotoxicity of UCNPs and the UCNPs@Dopamine−Melanin Hybrid System. In order to facilitate the potential utility of UCNPs@dopamine-melanin hybrid composites as bioprobes or theranostic nanocarriers in vivo, the cytotoxicity of UCNPs and UCNPs@dopamine−melanin nanocomposites was tested on Hela cells by MTT assay. The viability of nontreated Hela cells was set as 100%, and the viability of NP-treated Hela cells was calculated accordingly. After incubation for 24 h, a high cell viability (>90%) was measured even with the concentrations of UCNPs and UCNPs@dopamine−melanin nanocomposites as high as 640 μg/mL (Figure S7 in the SI). It is worth mentioning that the lower cytotoxicity of UCNPs@dopamine−melanin nanocomposites than UCNPs at the same concentration demonstrates the biocompatibility of dopamine−melanin shells formed by self-polymerization of dopamine, suggesting the use of UCNPs@dopamine−melanin nanocomposites as potential bioprobes for intracellular sensing or in vivo real-time monitoring.

Antioxidant Capacity Assay of Cell Extracts. The lysate of Hela cells was used as a representative biological sample for antioxidant capacity evaluation using the developed sensing platform. As known, biothiols account for a large portion of the intracellular antioxidant capacity, especially considering the activity of the thiol groups in their Cys moiety. In this study, the antioxidant capacity of cell extracts was determined using the Cys calibration curve (Figure 6C) as a standard, and the results were presented as Cys-equivalent antioxidant capacity (CEAC). Because GSH shows a high concentration inside the cells and plays an essential role in maintaining the redox state of the cells, buthionine sulfoximine (BSO, a glutathione synthesis inhibitor) and α-lipoic acid (LPA, a GSH synthesis enhancer) were preincubated with Hela cells to disturb the intracellular glutathione level and to further study the sensitivity of the sensing platform for glutathione interference. The upconversion fluorescence intensities of the UCNPs@dopamine−melanin hybrid system with three different lysed Hela cell samples and a blank control are shown in Figure 9A. Compared to a normal Hela cell sample, the lysate with BSO showed an obvious decrease of the fluorescence intensity, while the cells treated with LPA exhibited a noticeable increase. The CEAC value for each sample was compared directly in Figure 9B and summarized in Table 1. The CEACs of nontreated, BSO-treated, and LPA-treated Hela cells were determined to be 13.65 ± 0.91, 6.82 ± 0.92, and 17.93 ± 1.11 μM (6×10^5 cells/mL), respectively. This result demonstrated the capability of the developed sensing platform for detection of the intracellular

Table 1. Performance of the UCNPs@Dopamine−Melanin Hybrid System in Antioxidant Capacity Assay of Deproteinized Human Plasma and Hela Cell Extract Samples

	determined antioxidant[a] (μM, Cys equiv)			
sample	without spiking	5 μM Cys spiked	recovery (%)	RSD (%, n = 3)
10% Plasma-1	65.16 ± 2.67	69.84 ± 2.83	94.08	4.05
10% Plasma-2	55.58 ± 2.01	60.36 ± 2.05	95.64	3.40
10% Plasma-3	48.46 ± 3.01	53.56 ± 3.04	100.08	5.69
Hela cell (normal)	13.65 ± 0.91	18.30 ± 0.94	92.93	5.08
Hela cell (+BSO)	6.82 ± 0.92	11.26 ± 1.52	96.47	8.57
Hela cell (+LPA)	17.93 ± 1.11	23.50 ± 1.69	111.33	4.74

[a]Mean value of three independent measurements. The antioxidants were determined by using the Cys calibration curve as the standard, and the results are presented as CEAC. The given value in the table = 6 × determined value because samples were tested by adding 0.5 mL of diluted plasma or cell extracts into 2.5 mL of the UCNPs@dopamine−melanin hybrid system.

DOI: 10.1021/am5086269
ACS Appl. Mater. Interfaces 2015, 7, 3030−3040

antioxidant capacity changes in response to various conditions. In addition, known amounts of Cys were added to the three lysed cell samples (nontreated, BSO, and LPA), and satisfactory Cys recovery values were all obtained, with relative standard deviation (RSD) values of less than 9%. Taken together, these results support the feasibility of using the UCNPs@dopamine−melanin hybrid system for intracellular CEAC monitoring.

Antioxidant Capacity Assay of Human Plasma. Evaluation of the antioxidant capacity was also performed on the diluted deproteinized human plasma. The proteins in plasma were removed to reduce the effect of the fluid viscosity on the aggregation of UCNPs. As shown in Figure S8A in the SI, the whole blood, the deproteinized plasma, and the extract of deproteinized red blood cells all show strong absorption spans visible to the UV region, causing unwanted background interference in colorimetric measurement. With 980 nm NIR excitation, no fluorescence background from human plasma was measured in the entire visible region, while a high fluorescence background from plasma was measured under UV or near UV (350 or 488 nm) excitation (Figure S8B in the SI). Thus, fluorescence background interference could be successfully avoided on the UCNPs for antioxidant capacity assay. For easy analysis, the antioxidant capacity of human plasma was also determined by using Cys as the reference, and the results are given as CEAC. The CEACs of three plasma samples are 65.16 ± 2.67, 55.58 ± 2.01, and 48.46 ± 3.01 μM (10% deproteinized human plasma; Table 1).

Recoveries of the known spiked amounts of Cys were between 94.1% and 100.1% with a satisfactory precision. Previous studies have shown that the concentration of Cys in human serum is 160−330 μM,[56] and the CEAC obtained by this UCNPs@dopamine−melanin hybrid system assay was obviously higher (about twice) than the normal amount of Cys in human plasma. The total antioxidant capacity of human plasma comes from the collective activities of various antioxidative substances and their cooperation.[8] The obtained CEAC value may reflect the summation of the main antioxidant activities in the plasma but may not account for the total antioxidant capacity due to the removal of proteins. Furthermore, no single method is capable of detecting all components of the antioxidant capacity in serum or other body fluids, and there is no "gold standard" yet for total antioxidant capacity measurement.[9,12] A large amount of endogenous antioxidants have shown an inhibitory characteristic for melanin synthesis, which is the inspiration for the basis of this study. Taken together, the results demonstrate the applicability and reliability of the bioinspired UCNPs@dopamine−melanin hybrid system for antioxidant capacity evaluation of human plasma or other biological fluids.

CONCLUSIONS

In conclusion, dopamine−melanin nanoshells could be easily formed on the surface of UCNPs in an alkaline solution through the spontaneous oxidative polymerization of dopamine. These dopamine−melanin nanoshells acted as ultra-efficient quenchers for the upconversion nanophosphors, and the quenching effect could be effectively inhibited by the presence of various antioxidants. Taking advantage of the highly sensitive spontaneous oxidative and antioxidative reaction, the unique fluorescence quenching property of dopamine−melanin, and the free background interference feature offered by NIR excitation, a facile NIR-excited UNACA platform has been developed and further used to evaluate the antioxidant capacity in cell extracts and human plasma. Satisfactory specificity and repeatability were achieved. Together with the enhanced sensitivity under NIR excitation for real biological sample assay, this UCNPs@dopamine−melanin hybrid system represents a practical platform for screening and quantitative evaluation of the antioxidants in biological samples and a promising tool for investigation of the relationship of free oxygen radicals and the endogenous antioxidative defense system.

EXPERIMENTAL SECTION

Materials. Lanthanide chlorides ($YCl_3·6H_2O$, $YbCl_3·6H_2O$, $ErCl_3·6H_2O$, 99.99%), sodium trifluoroacetate (98%), 1-octadecene (ODE, 90%), oleic acid (OA, 90%), and dopamine hydrochloride (98%) were purchased from J&K Chemical Co., Ltd. (Beijing, China). Reduced glutathione (GSH), cysteine (Cys), homocysteine (Hcy), L-glutathione oxidized (GSSG), L-ascorbic acid (AA or Vc), Trolox, glucose, and all of the other 19 amino acids were purchased from Aladdin Reagent Co., Ltd. (Shanghai, China). α-Lipoic acid (LPA), buthionine sulfoximine (BSO), and 3-(4,5-dimethylthiazol-2-yl)-2,5-diphenyltetrazolium bromide (MTT) were purchased from Sigma-Aldrich Co., Ltd. (Shanghai, China). Tris(hydroxymethyl)aminomethane (Tris), hydrochloric acid (HCl, 38%), dimethyl sulfoxide (DMSO), diethylene glycol (DEG), trisodium citrate, ethanol, and chloroform were purchased from Sinopharm Chemical Reagent Co., Ltd. (Shanghai, China). Double-distilled deionized water was used throughout the experiments. All of the chemicals employed were used without further purification.

Synthesis of $NaYF_4$:Yb,Er UCNPs. $NaYF_4$:Yb,Er UCNPs were synthesized by a solvothermal procedure. In brief, 0.8 mmol of $YCl_3·6H_2O$, 0.18 mmol of $YbCl_3·6H_2O$, and 0.02 mmol of $ErCl_3·6H_2O$ were initially dissolved completely in 6 mL of OA and 15 mL of ODE at 160 °C under vacuum for 1 h. Then the solution was cooled to room temperature naturally, followed by the addition of 2.5 mmol of sodium trifluoroacetate. The temperature of the solution was increased to 320 °C and maintained for 1 h under a nitrogen flow. After cooling to room temperature naturally, precipitates were obtained via centrifugation and were washed with ethanol/water/cyclohexane (1:1:2) three times. The product was dried under vacuum at 80 °C for 24 h before use.

Surface Hydrophilic Modification of $NaYF_4$:Yb,Er UCNPs. Trisodium citrate was used as the surface ligand to get hydrophilic UCNPs: 100 mg of UCNPs was dispersed in 60 mL of DEG, and 200 mg of trisodium citrate was added to the solution. The mixed solution was sealed and heated to 200 °C with gentle agitation. After the reaction finished and cooled to room temperature, 20 mL of 0.1 M diluted HCl was added to wash the product. Hydrophilic UCNPs were collected by centrifugation, the washing/centrifugation procedure was repeated three times, and the final product was dried by freeze-drying.

Fluorescence Quenching and Antiquenching Investigation. To investigate the fluorescence quenching effect of the spontaneous oxidation of dopamine to UCNPs, dopamine hydrochloride with different final concentrations (0, 0.25, 5, 10, and 20 mM) was added to 3 mL of a UCNPs (0.2 mg/mL) and Tris-HCl buffer (10 mM, pH 8.5) solution. The mixture was incubated at room temperate under gentle vortex mixing. With a 10 min time interval, the sample solution was taken to characterize by UV−vis absorption spectroscopy, 980 nm NIR-excited upconversion fluorescence spectroscopy, and TEM. In the antiquenching experiments, GSH (0, 20, and 40 μM) was added to the solution before the addition of dopamine hydrochloride. Then, the sample solution was characterized at a series of time points by UV−vis absorption and upconversion fluorescence spectroscopy.

Antioxidant Capacity Assay in Aqueous Solution. In a typical GSH detection procedure using the UCNPs@dopamine−melanin hybrid system, 500 μL of a GSH aqueous solution with an increasing final concentration (0−30 μM) was incubated with a fixed amount of UCNPs (0.2 mg/mL) in a set of tubes, adjusting the total volume to 3 mL with a Tris-HCl (10 mM, pH 8.5) buffer. Then, a fixed amount of

DOI: 10.1021/am5086269
ACS Appl. Mater. Interfaces 2015, 7, 3030−3040

dopamine hydrochloride (5 mM) was added to the mixture and further incubated at room temperate under gentle vortex mixing. After 30 min of reaction, 10 μL of a HCl solution (120 mM) was added to the solution to block the reaction before fluorescence measurement. The fluorescence emission spectra and intensity at 540 nm were measured at an excitation wavelength of 980 nm. Analysis of other antioxidants, such as Cys, Vc, Trolox, Hcy, etc., followed the same process, except replacing the GSH with 500 μL of other antioxidant aqueous solutions. To examine the specificity of the UCNPs@dopamine−melanin hybrid system toward antioxidants, 100-fold excess of glucose, GSSG, and other amino acids were added into the control samples in place of GSH, following an identical procedure. To test the response performance of this sensing platform toward a multicomponent environment, 76% Cys + 20% Vc + 4% GSH was diluted into a MEM cell culture medium, and the sample (with a final concentration of 25 μM) was taken to conduct the specificity test following the same protocol.

Cell Culture and Cytotoxicity of UCNPs and the UCNPs@Dopamine−Melanin System. Hela cells were maintained at 37 °C in 5% CO_2 in the DMEM media supplemented with 10% fetal calf serum, 100 U/mL penicillin, and 100 mg/mL streptomycin. In vitro cytotoxicity to Hela cells was determined by MTT assay. Briefly, Hela cells were seeded in a 96-well plate at 1×10^4/well and incubated for 12 h. Then UCNPs and UCNPs@dopamine−melanin colloid solutions at different concentrations (0, 10, 20, 40, 80, 160, 320, and 640 μg/mL, diluted in DMEM) were added into the 96-well plate. Subsequently, the 96-well plate was cultured for 24 h prior to MTT assay. Upon incubation with a MTT solution (1 mg/mL) for 4 h, 100 μL of DMSO was added to each well to extract formazon for 30 min. The absorbance of the resulting solutions was measured at 570 nm using a microplate reader (BioRad 680, Hercules, CA). The cell viability was presented as the percentage of control samples. Three independent experiments in duplicate were performed.

Antioxidant Capacity Assay of Cell Extracts. The Hela cells were plated at around 50−60% confluency 36 h before antioxidant assay experiments in 35 mm culture dishes. Prior to antioxidant assay experiments, the Hela cells were treated with LPA (a GSH synthesis enhancer, 500 μM) for 24 h and BSO (a glutathione synthesis inhibitor, 100 μM) for 4 h. These two groups were set as control groups. All three groups of cells were collected and washed three times with a PBS buffer and then suspended in a PBS buffer. The cell number for each group was adjusted to the same value (1×10^7/mL) by cell counting. The cells were further lysed with sonication to release antioxidants from the cells. After that, twice the volume of absolute methanol was added to the lysed cells with shaking, the proteins and fragments were precipitated and removed by centrifugation, the supernatant was collected and diluted with PBS to proper concentration, and 500 μL of each diluted cell extract was then analyzed using the procedure described above. (The final concentration of the cells was equivalent to 1×10^5 cells/mL.) For the antioxidant recovery assay in cell extracts, the assay solution was spiked with a known concentration of Cys, and the total quantities of Cys recovery, the recovery rates, and the standard deviation values were obtained (Table 1).

Antioxidant Capacity Assay in Human Plasma. The human whole blood samples stored in vacuum blood collection tubes were obtained from the Department of Blood Transfusion, Xiamen Maternity & Child Health Care Hospital (Xiamen, China), and assayed as soon as possible after collection. For each test, 3 mL of the blood sample was transferred into Eppendorf tubes and centrifuged at 4000 rpm for 5 min at room temperature to remove cells and platelets, and then 1 mL of supernatant plasma was taken out and diluted to a 4 mL solution with PBS for further use. Afterward, 6 mL of absolute methanol was added to the diluted plasma with shaking for 3 min, and plasma proteins were precipitated and removed by centrifugation. The supernatant was collected to get 10% deproteinized human plasma, and 500 μL of each 10% diluted plasma sample was then taken for analysis using the same procedure as that described above. For the antioxidant recovery assay in human plasma, the assay solution was spiked with a known concentration of Cys, and the total quantities of Cys recovery, the recovery rates, and the standard deviation values were obtained (Table 1).

Instruments and Characterization. An XRD system (X'pert Pro, PANalytical Co., Almelo, The Netherlands) with Cu Kα radiation (λ = 1.5406 Å) was used for characterization of the phase purity and crystallinity of the samples. The size and morphology of the samples were obtained by a transmission electron microscope (JEM-2100, JEOL, Tokyo, Japan) operated at an accelerating voltage of 200 kV. Samples were prepared by dripping a drop of the nanocrystal dispersion in cyclohexane or in deionized water onto the surface of holey copper grids and allowing it to dry in air at room temperature. The FT-IR spectra were obtained on a Magan-IR spectrometer 500 (Nicolet, Madison, WI) with the KBr pellet technique. The surface ζ potential of the trisodium citrate modified UCNPs was measured by a Zetasizer Nano ZS (Malvern Instruments Ltd., Malvern, U.K.). UV−vis absorption spectra were acquired with a DU 800 UV−vis spectrophotometer (Beckman Coulter, Fullerton, CA). The upconversion emission spectra were obtained by using a Fluoromax-4 spectrofluorometer (Horiba Jobin Yvon, Longjumeau, France), with an external 980 nm laser diode (1.3 W, Beijing Hi-Tech Optoelectronic Co., Beijing, China) as the excitation source instead of the internally equipped lamp. Digital photographs were taken with a Sony NEX-5R camera.

■ ASSOCIATED CONTENT

Supporting Information

TEM image and XRD pattern of $NaYF_4$:Yb,Er UCNPs synthesized by the solvothermal procedure, FT-IR spectra of UCNPs before and after surface hydrophilic modification, surface ζ potential of hydrophilic UCNPs, comparison of the different dopamine oxidation inhibition activities between Trolox and AA, nonlinear fitted curves of the antiquenching efficiency as a function of the concentration of GSH, Cys, or Vc, cytotoxicity of UCNPs and a UCNPs@dopamine−melanin hybrid system, UV−vis absorption spectra of the whole blood, the deproteinized plasma, and the deproteinized red blood cell extract samples, and fluorescence emission spectra of the deproteinized plasma under 350, 488, and 980 nm excitation. This material is available free of charge via the Internet at http://pubs.acs.org.

■ AUTHOR INFORMATION

Corresponding Author

*E-mail: renlei@xmu.edu.cn. Tel: +86 592 2188530. Fax: +86 592 2183937.

Author Contributions

§D.W. and C.C. contributed equally. The manuscript was written through contributions of all authors. All authors have given approval to the final version of the manuscript.

Notes

The authors declare no competing financial interest.

■ ACKNOWLEDGMENTS

This work was financially supported by the National Basic Research Program of China (973 Program; Grant 2013CB933703), the National Nature Science Foundation of China (Grants 31371012 and 81171448), and the Medical Science and Technology Innovation Program of Nanjing Military Region (11Z022).

■ REFERENCES

(1) Sies, H. *Oxidative Stress*; Academic Press: London, 1985.
(2) Pham-Huy, L. A.; He, H.; Pham-Huy, C. Free Radicals, Antioxidants in Disease and Health. *Int. J. Biomed. Sci.* **2008**, *4*, 89−96.

DOI: 10.1021/am5086269
ACS Appl. Mater. Interfaces 2015, 7, 3030−3040

(3) Singh, U.; Jialal, I. Oxidative Stress and Atherosclerosis. *Pathophysiology* **2006**, *13*, 129−142.
(4) Guidi, I.; Galimberti, D.; Lonati, S.; Novembrino, C.; Bamonti, F.; Tiriticco, M.; Fenoglio, C.; Venturelli, E.; Baron, P.; Bresolin, N. Oxidative Imbalance in Patients with Mild Cognitive Impairment and Alzheimer's Disease. *Neurobiol. Aging* **2006**, *27*, 262−269.
(5) Smith, M. A.; Rottkamp, C. A.; Nunomura, A.; Raina, A. K.; Perry, G. Oxidative Stress in Alzheimer's Disease. *Biochim. Biophys. Acta, Mol. Basis Dis.* **2000**, *1502*, 139−144.
(6) Bolton, J. L.; Trush, M. A.; Penning, T. M.; Dryhurst, G.; Monks, T. J. Role of Quinones in Toxicology. *Chem. Res. Toxicol.* **2000**, *13*, 135−160.
(7) Kinnula, V. L.; Crapo, J. D. Superoxide Dismutases in Malignant Cells and Human Tumors. *Free Radical Biol. Med.* **2004**, *36*, 718−744.
(8) Halliwell, B. Antioxidants: The Basics—What They are and How to Evaluate Them. *Adv. Pharmacol.* **1997**, *38*, 3−20.
(9) Niki, E. Assessment of Antioxidant Capacity in Vitro and in Vivo. *Free Radical Biol. Med.* **2010**, *49*, 503−515.
(10) Joshipura, K. J.; Hu, F. B.; Manson, J. E.; Stampfer, M. J.; Rimm, E. B.; Speizer, F. E.; Colditz, G.; Ascherio, A.; Rosner, B.; Spiegelman, D. The Effect of Fruit and Vegetable Intake on Risk for Coronary Heart Disease. *Ann. Int. Med.* **2001**, *134*, 1106−1114.
(11) Riboli, E.; Norat, T. Epidemiologic Evidence of the Protective Effect of Fruit and Vegetables on Cancer Risk. *Am. J. Clin. Nutr.* **2003**, *78*, 559S−569S.
(12) Badarinath, A.; Rao, K. M.; Chetty, C. M. S.; Ramkanth, S.; Rajan, T.; Gnanaprakash, K. A Review on in Vitro Antioxidant Methods: Comparisions, Correlations and Considerations. *Int. J. PharmTech Res.* **2010**, *2*, 1276−1285.
(13) Alam, M. N.; Bristi, N. J.; Rafiquzzaman, M. Review on in Vivo and in Vitro Methods Evaluation of Antioxidant Activity. *Saudi Pharm. J.* **2013**, *21*, 143−152.
(14) Rice-Evans, C.; Miller, N. J. Total Antioxidant Status in Plasma and Body Fluids. *Methods Enzymol.* **1994**, *234*, 279−293.
(15) Chanda, S.; Dave, R. In vitro Models for Antioxidant Activity Evaluation and Some Medicinal Plants Possessing Antioxidant Properties: an Overview. *Afr. J. Microbiol. Res.* **2009**, *3*, 981−996.
(16) Benzie, I. F.; Strain, J. The Ferric Reducing Ability of Plasma (FRAP) as a Measure of "Antioxidant Power": the FRAP Assay. *Anal. Biochem.* **1996**, *239*, 70−76.
(17) Cao, G.; Alessio, H. M.; Cutler, R. G. Oxygen-radical Absorbance Capacity Assay for Antioxidants. *Free Radical Biol. Med.* **1993**, *14*, 303−311.
(18) Wayner, D.; Burton, G.; Ingold, K.; Locke, S. Quantitative Measurement of the Total, Peroxyl Radical-trapping Antioxidant Capability of Human Blood Plasma by Controlled Peroxidation. The Important Contribution Made by Plasma Proteins. *FEBS Lett.* **1985**, *187*, 33−37.
(19) Shen, J.; Sun, L. D.; Yan, C. H. Luminescent Rare Earth Nanomaterials for Bioprobe Applications. *Dalton Trans.* **2008**, *14*, 5687−5697.
(20) Tian, D.; Qian, Z.; Xia, Y.; Zhu, C. Gold Nanocluster-based Fluorescent Probes for Near-infrared and Turn-on Sensing of Glutathione in Living Cells. *Langmuir* **2012**, *28*, 3945−3951.
(21) Vilela, D.; González, M. C.; Escarpa, A. Nanoparticles as Analytical Tools for in Vitro Antioxidant Capacity Assessment and Beyond. *TrAC, Trends Anal. Chem.* **2015**, *64*, 1−16.
(22) Scampicchio, M.; Wang, J.; Blasco, A. J.; Sanchez Arribas, A.; Mannino, S.; Escarpa, A. Nanoparticle-based Assays of Antioxidant Activity. *Anal. Chem.* **2006**, *78*, 2060−2063.
(23) Li, H.; Ma, X.; Dong, J.; Qian, W. Development of Methodology Based on the Formation Process of Gold Nanoshells for Detecting Hydrogen Peroxide Scavenging Activity. *Anal. Chem.* **2009**, *81*, 8916−8922.
(24) Özyürek, M.; Güngör, N.; Baki, S.; Güçlü, K.; Apak, R. a. Development of a Silver Nanoparticle-based Method for the Antioxidant Capacity Measurement of Polyphenols. *Anal. Chem.* **2012**, *84*, 8052−8059.
(25) Zou, G.; Ju, H. Electrogenerated Chemiluminescence from a CdSe Nanocrystal Film and its Sensing Application in Aqueous Solution. *Anal. Chem.* **2004**, *76*, 6871−6876.
(26) Jiang, H.; Ju, H. Electrochemiluminescence Sensors for Scavengers of Hydroxyl Radical Based on its Annihilation in CdSe Quantum Dots Film/peroxide System. *Anal. Chem.* **2007**, *79*, 6690−6696.
(27) Anker, J. N.; Hall, W. P.; Lyandres, O.; Shah, N. C.; Zhao, J.; Van Duyne, R. P. Biosensing with Plasmonic Nanosensors. *Nat. Mater.* **2008**, *7*, 442−453.
(28) Yi, G.; Lu, H.; Zhao, S.; Ge, Y.; Yang, W.; Chen, D.; Guo, L. H. Synthesis, Characterization, and Biological Application of Size-controlled Nanocrystalline $NaYF_4$: Yb, Er Infrared-to-visible Upconversion Phosphors. *Nano Lett.* **2004**, *4*, 2191−2196.
(29) Heer, S.; Kömpe, K.; Güdel, H. U.; Haase, M. Highly Efficient Multicolour Upconversion Emission in Transparent Colloids of Lanthanide-Doped $NaYF_4$ Nanocrystals. *Adv. Mater.* **2004**, *16*, 2102−2105.
(30) Wang, D.; Ren, L.; Zhou, X.; Wang, X.; Zhou, J.; Han, Y.; Kang, N. Rapid Microwave-enhanced Hydrothermal Synthesis and Shape Evolution of Uniform $NaGdF_4$:Yb,Er (Tm/Ho) Nanocrystals with Upconversion and Paramagnetic Properties. *Nanotechnology* **2012**, *23*, 225705.
(31) Frangioni, J. V. In vivo Near-infrared Fluorescence Imaging. *Curr. Opin. Chem. Biol.* **2003**, *7*, 626−634.
(32) Nyk, M.; Kumar, R.; Ohulchanskyy, T. Y.; Bergey, E. J.; Prasad, P. N. High Contrast in Vitro and in Vivo Photoluminescence Bioimaging Using Near Infrared to Near Infrared Upconversion in Tm^{3+} and Yb^{3+} Doped Fluoride Nanophosphors. *Nano Lett.* **2008**, *8*, 3834−3838.
(33) Chatterjee, D.; Rufaihah, A.; Zhang, Y. Upconversion Fluorescence Imaging of Cells and Small Animals Using Lanthanide Doped Nanocrystals. *Biomaterials* **2008**, *29*, 937−943.
(34) Liu, C.; Wang, Z.; Jia, H.; Li, Z. Efficient Fluorescence Resonance Energy Transfer between Upconversion Nanophosphors and Graphene Oxide: a Highly Sensitive Biosensing Platform. *Chem. Commun.* **2011**, *47*, 4661−4663.
(35) Ding, Y.; Zhu, H.; Zhang, X.; Zhu, J. J.; Burda, C. Rhodamine B Derivative-functionalized Upconversion Nanoparticles for FRET-based Fe^{3+}-sensing. *Chem. Commun.* **2013**, *49*, 7797−7799.
(36) Wang, M.; Hou, W.; Mi, C. C.; Wang, W. X.; Xu, Z. R.; Teng, H. H.; Mao, C. B.; Xu, S. K. Immunoassay of Goat Antihuman Immunoglobulin G Antibody Based on Luminescence Resonance Energy Transfer between Near-Infrared Responsive $NaYF_4$:Yb,Er Upconversion Fluorescent Nanoparticles and Gold Nanoparticles. *Anal. Chem.* **2009**, *81*, 8783−8789.
(37) Deng, R.; Xie, X.; Vendrell, M.; Chang, Y. T.; Liu, X. Intracellular Glutathione Detection Using MnO_2-nanosheet-modified Upconversion Nanoparticles. *J. Am. Chem. Soc.* **2011**, *133*, 20168−20171.
(38) Swan, G. Chemical Structure of Melanins. *Ann. N.Y. Acad. Sci.* **1963**, *100*, 1005−1019.
(39) Meredith, P.; Riesz, J. Radiative Relaxation Quantum Yields for Synthetic Eumelanin. *Photochem. Photobiol.* **2004**, *79*, 211−216.
(40) Ryu, J.; Park, H. Y.; Kim, K.; Kim, H.; Yoo, J. H.; Kang, M.; Im, K.; Grailhe, R.; Song, R. Facile Synthesis of Ultrasmall and Hexagonal $NaGdF_4$:Yb^{3+},Er^{3+} Nanoparticles with Magnetic and Upconversion Imaging Properties. *J. Phys. Chem. C* **2010**, *114*, 21077−21082.
(41) Cao, T.; Yang, T.; Gao, Y.; Yang, Y.; Hu, H.; Li, F. Water-soluble $NaYF_4$:Yb/Er Upconversion Nanophosphors: Synthesis, Characteristics and Application in Bioimaging. *Inorg. Chem. Commun.* **2010**, *13*, 392−394.
(42) Lee, H.; Dellatore, S. M.; Miller, W. M.; Messersmith, P. B. Mussel-inspired Surface Chemistry for Multifunctional Coatings. *Science* **2007**, *318*, 426−430.
(43) Burda, C.; Green, T.; Link, S.; El-Sayed, M. Electron Shuttling Across the Interface of CdSe Nanoparticles Monitored by Femtosecond Laser Spectroscopy. *J. Phys. Chem. B* **1999**, *103*, 1783−1788.

DOI: 10.1021/am5086269
ACS Appl. Mater. Interfaces 2015, 7, 3030−3040

(44) Medintz, I. L.; Stewart, M. H.; Trammell, S. A.; Susumu, K.; Delehanty, J. B.; Mei, B. C.; Melinger, J. S.; Blanco-Canosa, J. B.; Dawson, P. E.; Mattoussi, H. Quantum-dot/dopamine Bioconjugates Function as Redox Coupled Assemblies for in Vitro and Intracellular pH Sensing. *Nat. Mater.* **2010**, *9*, 676−684.
(45) Nofsinger, J. B.; Forest, S. E.; Simon, J. D. Explanation for the Disparity among Absorption and Action Spectra of Eumelanin. *J. Phys. Chem. B* **1999**, *103*, 11428−11432.
(46) Nofsinger, J. B.; Ye, T.; Simon, J. D. Ultrafast Nonradiative Relaxation Dynamics of Eumelanin. *J. Phys. Chem. B* **2001**, *105*, 2864−2866.
(47) Ji, X.; Palui, G.; Avellini, T.; Na, H. B.; Yi, C.; Knappenberger, K. L., Jr.; Mattoussi, H. On the pH-dependent Quenching of Quantum Dot Photoluminescence by Redox Active Dopamine. *J. Am. Chem. Soc.* **2012**, *134*, 6006−6017.
(48) Scott, D. T.; McKnight, D. M.; Blunt-Harris, E. L.; Kolesar, S. E.; Lovley, D. R. Quinone Moieties Act as Electron Acceptors in the Reduction of Humic Substances by Humics-reducing Microorganisms. *Environ. Sci. Technol.* **1998**, *32*, 2984−2989.
(49) Ye, T.; Simon, J. D.; Sarna, T. Ultrafast Energy Transfer from Bound Tetra (4-*N*,*N*,*N*,*N*-trimethylanilinium)porphyrin to Synthetic Dopa and Cysteinyldopa Melanins. *Photochem. Photobiol.* **2003**, *77*, 1−4.
(50) Qiang, W.; Li, W.; Li, X.; Chen, X.; Xu, D. Bioinspired Polydopamine Nanospheres: a Superquencher for Fluorescence Sensing of Biomolecules. *Chem. Sci.* **2014**, *5*, 3018−3024.
(51) Bernsmann, F.; Ponche, A.; Ringwald, C.; Hemmerlé, J.; Raya, J.; Bechinger, B.; Voegel, J. C.; Schaaf, P.; Ball, V. Characterization of Dopamine−melanin Growth on Silicon Oxide. *J. Phys. Chem. C* **2009**, *113*, 8234−8242.
(52) Ju, K. Y.; Lee, Y.; Lee, S.; Park, S. B.; Lee, J. K. Bioinspired Polymerization of Dopamine to Generate Melanin-like Nanoparticles Having an Excellent Free-radical-scavenging Property. *Biomacromolecules* **2011**, *12*, 625−632.
(53) Matsuki, M.; Watanabe, T.; Ogasawara, A.; Mikami, T.; Matsumoto, T. Inhibitory Mechanism of Melanin Synthesis by Glutathione. *Yakugaku Zasshi* **2008**, *128*, 1203−1207.
(54) Shimada, Y.; Tai, H.; Tanaka, A.; Ikezawa-Suzuki, I.; Takagi, K.; Yoshida, Y.; Yoshie, H. Effects of Ascorbic Acid on Gingival Melanin Pigmentation in Vitro and in Vivo. *J. Periodontol.* **2009**, *80*, 317−323.
(55) Khaw, K. T.; Woodhouse, P. Interrelation of Vitamin C, Infection, Haemostatic Factors, and Cardiovascular Disease. *Br. Med. J.* **1995**, *310*, 1559−1563.
(56) Jacobsen, D. W.; Gatautis, V. J.; Green, R.; Robinson, K.; Savon, S. R.; Secic, M.; Ji, J.; Otto, J. M.; Taylor, L. Rapid HPLC Determination of Total Homocysteine and Other Thiols in Serum and Plasma: Sex Differences and Correlation with Cobalamin and Folate Concentrations in Healthy Subjects. *Clin. Chem.* **1994**, *40*, 873−881.

DOI: 10.1021/am5086269
ACS Appl. Mater. Interfaces 2015, 7, 3030−3040